Front. Earth Sci. 2023, 17(1): 262–272
https://doi.org/10.1007/s11707-022-0976-3

RESEARCH ARTICLE

Effects of coal molecular structure and pore morphology on methane adsorption and accumulation mechanism

Jingshuo ZHANG, Xiaoming NI (✉), Ying HAN, Junfeng LIN

School of Energy Science and Engineering, Henan Polytechnic University, Jiaozuo 454000, China

Abstract The adsorption, diffusion, and aggregation of methane from coal are often studied based on slit or carbon nanotube models and isothermal adsorption and thermodynamics theories. However, the pore morphology of the slit model involves a single slit, and the carbon nanotube model does not consider the molecular structure of coal. The difference of the adsorption capacity of coal to methane was determined without considering the external environmental conditions by the molecular structure and pore morphology of coal. The study of methane adsorption by coal under single condition cannot reveal its mechanism. In view of this, elemental analysis, FTIR spectrum, XPS electron energy spectrum, ^{13}C NMR, and isothermal adsorption tests were conducted on the semi-anthracite of Changping mine and the anthracite of Sihe Mine in Shanxi Province, China. The grand canonical Monte Carlo (GCMC) and molecular dynamics simulation method was used to establish the coal molecular structure model. By comparing the results with the experimental test results, the accuracy and practicability of the molecular structure model are confirmed. Based on the adsorption potential energy theory and aggregation model, the adsorption force of methane on aromatic ring structure, pyrrole nitrogen structure, aliphatic structure, and oxygen-containing functional group was calculated. The relationship between pore morphology, methane aggregation morphology, and coal molecular structure was revealed. The results show that the adsorption force of coal molecular structure on methane is as follows: aromatic ring structure (1.96 kcal/mol) > pyridine nitrogen (1.41 kcal/mol) > pyrrorole nitrogen (1.05 kcal/mol) > aliphatic structure (0.29 kcal/mol) > oxygen-containing functional group (0.20 kcal/mol). In the long and narrow regular pores of semi-anthracite and anthracite, methane aggregates in clusters at turns and aperture changes, and the adsorption and aggregation positions are mainly determined by the aromatic ring structure, the positions of pyrrole nitrogen and pyridine nitrogen. The degree of aggregation is controlled by the interaction energy and pore morphology. The results pertaining to coal molecular structure and pore morphology on methane adsorption and aggregation location and degree are conducive to the evaluation of the adsorption mechanism of methane in coal.

Keywords Grand Canonical Monte Carlo, pore morphology, methane adsorption, molecular structure of coal

1 Introduction

Methane mainly occurs in coal in a state of adsorption, and the adsorption and diffusion behavior of coal to methane is jointly determined by the molecular structure of coal such as aromatic ring structure and fat structure, pore morphology, and external environment such as pressure and temperature (Meng et al., 2016; Tao et al., 2019). At present, scholars use carbon nanotube models, slit models, or aggregation models to study the adsorption, diffusion, and migration behavior of gas in the pore of its composition. When the carbon nanotubes model is applied to the study, more emphasis is placed on the influences of nano-pore structure, temperature, and pressure on gas viscosity, resulting in the influences of adsorption capacity and migration behavior. As the influence of coal molecular structure differences on methane adsorption behavior is not considered, so the research results are incomplete. When applying the slit model to research, staff in that particular laboratory tested the layer spacing and chemical structure composition of coal, and then constructed the slit model including the aromatic ring structure, fat structure and interlayer structure of coal. All the pores were regarded as slits, which were different from the real pore shape (Yeganegi

Received October 10, 2021; accepted February 17, 2022

E-mail: nxm1979@126.com

et al., 2016; Kazemi et al., 2017; Song et al., 2018; Tao et al., 2018). A state of aggregation model compensates for the nanotube model not considering defects in the molecular structure of the coal, and it can overcome the defect of the model of a single slit pore configuration. To study coal methane adsorption, giving full consideration to the coal molecular structure and the influences of pore morphology of methane adsorption behavior: based on this, according to the state of aggregation-model research, this research aims to examine the mechanism of coal methane adsorption.

In recent years, Mosher et al. (2013) verified the accuracy of the grand canonical Monte Carlo (GCMC) simulation method in nanoscale porous media through simulation and experimental comparisons. Li et al. (2018) compared the GCMC simulation results with the measurement results of adsorbed coal samples from two different coal mines using a laboratory gas absorption instrument, and investigated the adsorption characteristics of methane molecules on coal pores from different perspectives. Song et al. (2018) studied the relationship between excess isothermal adsorption lines, pore morphology, and adsorption capacity through GCMC simulations. The GCMC simulation method that is used to study the adsorption characteristics of methane molecules on coal pores has been gradually recognized by many scholars, so it is adopted in the present research.

To reveal the mechanism of methane adsorption by coal, the relationship between pore morphology, methane adsorption location, and molecular structure was studied. In this paper, elemental analysis, FTIR spectrum, XPS electron energy spectrum, ^{13}C NMR, and isothermal adsorption tests on semi-anthracite and anthracite were performed to construct the coal molecular structure model. The results were compared with the experimental test results (Liu et al., 2018; Zhao et al., 2018; Dong et al., 2019; Shang et al., 2019; Tao et al., 2020; Yan et al., 2020) to ensure the accuracy and availability of the established molecular structure model. The GCMC and molecular dynamics simulation method was used to assess methane adsorption on the aggregated coal molecular structure model, allowing observation of the morphology and composition of pores as well as the state of adsorption of methane molecules in the pores. The result lays a foundation for the study of the microscopic adsorption mechanism of coal to methane.

2 Research methods and procedures

2.1 Research methods

The research methods are described as follows.

1) Coal samples from Sihe Mine and Changping Mine (hereinafter referred to as SH coal and CP coal) in Shanxi Province were separately collected, and elemental analysis, ^{13}C NMR, FTIR, and XPS experiments were undertaken to establish the macromolecular structure model of coal.

Changping Mine is in Sizhuang Town, northwest of Gaoping City, in the southern Qinshui Basin. The main coal measures are 500—720 m of Taiyuan Formation of Upper Carboniferous and Shanxi Formation of Lower Permian. Sihe coal mine is in the south-east edge of Qinshui coalfield in the central and southern part of Shanxi Province. The coal bearing stratum is the No. 3 coal seam in the lower part of Shanxi Formation of Permian system, with a burial depth of about 450 m.

2) According to the coal high-pressure isothermal adsorption test method (GB/T 19560-2008), isothermal adsorption experiments were conducted on coal samples from the two mines.

3) According to the macromolecular structure model established, the isothermal adsorption curve of CH_4 adsorption could be simulated.

4) Microcosmic mechanisms of CH_4 adsorption by coal molecular structures were revealed.

The research method is as Fig. 1.

2.2 Research procedures

2.2.1 Establishing a molecular structure model for coal

1) According to coal industrial analysis method (GBT212-2008.), the SH and CP coal samples were subjected to elemental analysis.

2) The Bruker 600 MHz superconducting NMR spectrometer was used to perform ^{13}C NMR tests on coal samples. The ^{13}C NMR parameter table was obtained by means of peak separation fitting technique for the ^{13}C-spectrum after testing. The aromatic-ring structure in coal was determined by using the formula for the bridge carbon ratio, expressed as follows:

$$X_{BP} = f_a^B/(f_a^S + f_a^P + f_a^H), \quad (1)$$

where X_{BP} represents the ratio of aromatic bridgehead C to aromatic peripheral C on aromatic rings; f_a^B, f_a^S, f_a^P, and f_a^H denote aromatic bridgehead C, alkylated aromatic C, aromatic C bound to hydroxyl or ether oxygen, and protonated and aromatic C, respectively.

3) According to General Rules of Infrared Spectral Analysis (GB/T 6040-2019), FTIR test was conducted on coal samples from the two mines using an IS50-Seymour Flyer Spectrometer. Combined with ^{13}C NMR test results, the existing form of aliphatic structure in coal was determined.

4) According to general rules (GB/T19500-2004) for X-ray photoelectron spectroscopy analysis, XPS tests were conducted on coal samples from two mines using an AXIS ULTRA DLD X-ray photoelectron spectrometer, and according to the XPS test results, the distribution and

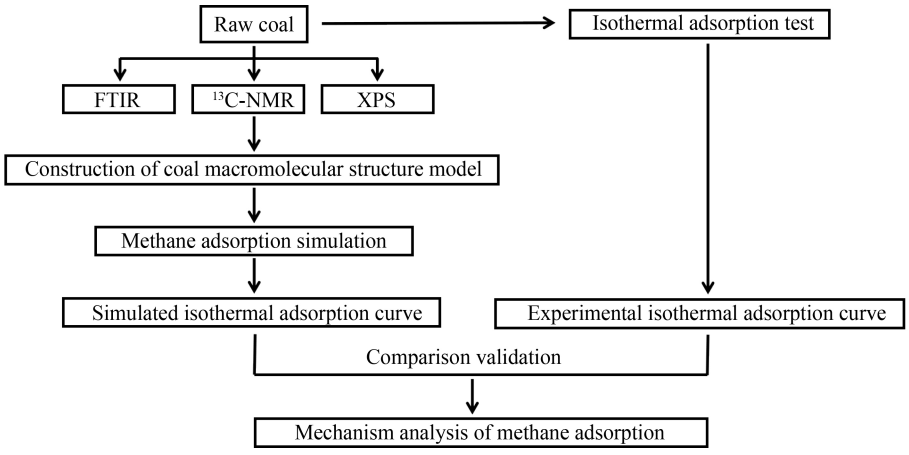

Fig. 1 Research methods.

proportion of each atomic structure form were determined by peak fitting.

5) After determining the composition of coal molecular structure, Materials Studio® modeling software was used to establish the coal molecular structure model. The specific construction method refers to published research (Bin et al., 2021).

The specific methods as follow.

1) Drawing of planar macromolecular structures and verification of calculated results

Step 1: According to the determined forms of aromatic hydrocarbons, aliphatic hydrocarbons, and heteroatoms in the coal samples, their chemical structures are obtained and drawn using the ACD/ChemSketch software.

Step 2: Chemical shifts of the drawn planar structures are calculated by using ACD/CNMR predictor, thus attaining the ^{13}C NMR spectra, which are then imported into Origin software for comparison with the experimental spectra to verify the accuracy of the calculated ^{13}C NMR spectra.

2) Model optimization

To make the established molecular structure model of coal better resemble the actual structures, molecular mechanics and molecular dynamics (annealing kinetics) in MS are used to optimize the planar macromolecular structures. The specific procedure is described as follows.

At first, the molecular dynamics simulation is performed to force the complex potential energy surface of macromolecular structures in coal to a state of local minimum energy. Then, the annealing process, comprising 10 cycles of heating or cooling by 5 K from the initial temperature of 300 K, with the highest temperature of 600 K, was conducted to determine the minimum energy and thereby optimize the structures, avoiding local minimization of the energy therein.

3) Isothermal adsorption experiments for coal

The ISO-300 isothermal adsorption apparatus was used to measure the absorption at 298.15 K, and eight pressure-points were used in these tests according to the high-pressure isothermal adsorption test method for coal (GB/T 19560-2008).

4) Simulation of CH_4 adsorption

(i) Optimization of the plane molecular structure model

The CH_4 molecular model was obtained using proprietary software, and the best matching molecular structure model was established by modifying the ^{13}C NMR atlas derived from experimental data.

(ii) Optimization of molecular mechanics and dynamics of the molecular structure model

The specific parameters of molecular mechanics are as follows: the maximum number of simulated loading steps was 100000, the number of process steps was set to 100000, the temperature cycle was run five times using automatic temperature control and automatic step adjustment; the quality was set to medium; the Metropolis calculation method was used, with the number of charge balance steps being 100000, and the force field set to the Dreiding force field model, which was cycled every 50 steps and averaged.

The molecular structure model was optimized by way of the “Dynamics” task in Forcite modules. First, the position of CH_4 adsorption was determined by using the adsorption locator modules in the software and the principle of simulated annealing in accordance with the principle of energy minimization. The initial rate followed a Boltzmann random distribution, and canonical ensemble (NVT) and Dreiding force fields were adopted (a Dreiding force field was found to be accurate and reliable than the Uff force field and COMPASS force field in predicting molecular systems composed of intramolar interaction forces. Therefore, the Dreiding force field was used in molecular mechanics, dynamics, and quantum mechanics simulations herein). Nose was employed to maintain the temperature at 298.15 K. The simulation was conducted for 3000 ps in increments of 0.5 fs, with output provided every 100 steps. The system reached equilibrium in the first 1500 ps, while the structural and dynamic properties of the system were obtained in the last 1500 ps.

5) Simulation of isothermal adsorption curves

The "Sorption isotherm" module in the software was used. The temperature was set to 298.15 K and the pressure ranged from 0 to 10 MPa (fugacity rather than pressure, had to be input to the software, and the pressure-fugacity conversion was realized by way of the Peng-Robinson equation). The GCMC simulation was based on periodic boundary conditions, and the initial configuration was a molecular structure model with the lowest energy and without adsorbate molecules. Thereafter, according to the change in energy, Metropolis operation rules were adopted to accept or reject the generation, disappearance, translation, and rotation of adsorbate molecules, so as to minimize the energy of the system and form a new configuration. The probabilities of accepting exchange of adsorbate molecules, configurational isomerization, rotation, and translation were 40%, 20%, 20%, and 20%, respectively.

6) Formula for pressure-fugacity conversion

The comparison state method is used to convert pressure to fugacity, and the formula is as follows (Du et al., 2021):

$$Z = \frac{PV}{RT}, \tag{2}$$

$$\ln\left(\frac{f}{P}\right) = \ln\varphi = \int_0^{P_r} \frac{Z-1}{P_r} \mathrm{d}P_r, \tag{3}$$

$$P_r = \frac{P}{P_c}, \tag{4}$$

where f, φ, R, and T represent the fugacity, dimensionless fugacity coefficient, ideal gas constant, and temperature, respectively; V, P, P_c, P_r, and Z represent the volume of gas, actual pressure, critical pressure strength (gas-liquid critical state), ratio of the real pressure to the critical pressure, and compression ratio, respectively.

2.2.2 Interaction energy between coal molecular structure and CH_4

1) Interaction energy between CH_4 molecules

For a pure adsorbate system, the L-J potential function was adopted to simulate the interaction between two CH_4 molecules (Sposito et al., 2000; Brochard et al., 2012; Wang et al., 2020; Men et al., 2021). Interaction energy ($E_{CH_4-CH_4}$) of the two in such a pure adsorption system depends on the distance r between the reference atoms:

$$E_{CH_4-CH_4}(r) = 4\varepsilon_{CH_4}\left[\left(\frac{\sigma_{CH_4}}{r}\right)^{12} - \left(\frac{\sigma_{CH_4}}{r}\right)^{6}\right], \tag{5}$$

where ε and σ denote the L-J parameters. Here L-J parameters proposed by Yohanes-Kurniawan et al. (2006) were used to calculate the density of CH_4 at the super critical conditions (T_c = 303.15 K and P_c = 4.62 MPa).

2) Interaction energy between coal structures

Interaction energy between the coal macro-molecules is modeled based on the following equation:

$$E_{coal-coal}(r) = \sum_{i\in coal} 4\varepsilon_{i-i}\left[\left(\frac{\sigma_{i-i}}{r_{i-i}}\right)^{12} - \left(\frac{\sigma_{i-i}}{r_{i-i}}\right)^{6}\right], \tag{6}$$

where ε_{i-i} and σ_{i-i} represent the L-J parameters between gas adsorbates and the atom i of coal depending on the nature of the atom i (C, H, N, or O). They can both be calculated by application of the Lorentz-Berthelot rules. The L-J parameters for the related atoms here are: σ_c = 3.36 Å, σ_H = 2.42 Å, σ_o = 3.033 Å, $\varepsilon_c = 28k_B$, $\varepsilon_H = 15.08k_B$, and $\varepsilon_o = 80.507k_B$.

3) Interaction energy between coal structure and CH_4

Interaction energy ($E_{CH_4\text{-}coal}$) between the gas adsorbates and coal macro-molecules is modeled based on the following equation:

$$E_{CH_4-coal} = E_{Total} - (E_{coal-coal} + E_{CH_4-CH_4}), \tag{7}$$

where E_{Total} (Etotal is calculated by the Forcite module) and $E_{coal\text{-}coal}$ represent the total energy of CH_4 adsorption by the coal molecular structure and the energy between coal molecular structures, respectively (i.e., the energy by which $E_{CH_4-CH_4}$ is adsorbed on CH_4 molecules).

3 Results and discussion

3.1 Establishment of the molecular structure model of coal

1) Results of elemental analysis

The results of elemental analysis are listed in Table 1.

2) Construction of the molecular structure model of coal

Among them, FTIR, XPS, and ^{13}C NMR analysis methods are all based on a peak-separation fitting method

Table 1 Test results of contents of main elements and $R_{o,max}$ of coal samples

Coal sample	Serial number	$R_{o,max}$%	Elemental analysis						
			C%	H%	N%	O%	S%	H/C	O/C
Changping mine coal	CP	2.68	88.91	3.77	1.91	4.98	0.43	0.51	0.04
Sihe mine coal	SH	3.28	91.06	3.13	1.58	3.71	0.52	0.41	0.03

Note: R_o is the average maximum vitrinite reflectance of coal.

(Tao et al., 2018; Meng et al., 2021). Parameters obtained by ^{13}C NMR are listed in Table 2.

The numbers of C, H, O, and N atoms were calculated using the results of elemental analysis, and the plane molecular structure models of CP and SH coal were preliminarily constructed. The molecular structure model of coal was modified by using matching experimental NMR spectra (Figs. 2 and 3). The element composition of the molecular structure model is summarized in Table 3.

3) Optimized molecular structure model

According to the optimization steps for molecular mechanics and dynamics of the molecular structure model (ii) in Step 4), optimized molecular structure models of CP semi-anthracite and SH anthracite are demonstrated in Figs. 4 and 5.

In the ball-and-stick model, gray represents carbon atoms; the white sphere represents hydrogen; the red ball denotes oxygen and the blue ball represents nitrogen atoms.

3.2 Comparison of coal isothermal adsorption experiments and simulation results

From the adsorption isotherm module, the fugacity-adsorption capacity curve of CH_4 adsorption by coal was obtained. Eqs. (2) to (4), used for pressure-fugacity conversion, were adopted to calculate the relationship between pressure and adsorption capacity. The simulation and experimentation results are shown in Fig. 6.

As illustrated in Fig. 6, the simulated behavior of CP and SH coal samples was aligned using a Langmuir model (The points in Fig. 6 are the pressure points set in the test simulation, and the curves in Fig. 6 are fitted accordingly). The simulated values of V_L for CP and SH coal samples are 37 and 43 cm^3/g. The values of V_L obtained experimentally are 34 and 42 cm^3/g. The simulated results are very close to the experimental results, which can therefore be analyzed according to the simulation.

Table 2 ^{13}C NMR parameters

Coal sample number	X_{BP}	f_a/%	f_a'/%	f_a^H/%	f_a^N/%	f_a^P/%	f_a^S/%	f_a^B/%	f_a^C/%	f_{al}/%	f_{al}*/%	f_{al}^H/%	f_{al}^O/%
CP	0.31	86.93	77.78	54.70	23.08	2.13	2.51	18.44	9.15	10.12	4.35	3.13	2.64
SH	0.36	80.33	73.25	47.68	25.57	2.93	3.22	19.42	7.08	14.62	4.68	3.95	5.99

Notes: f_a: total sp^2 hybridized C; f_{al}: total sp^3 hybridized C; f_a^C: carbonyl group or carboxyl group C ($\delta > 165$) ; f'_a: aromatic C; f_a^H: protonated and aromatic C ($100 \leqslant \delta \leqslant 129$); f_a^N: non-protonated and aromatic C; f_a^P: aromatic C bonded to hydroxyl or ether oxygen ($152 \leqslant \delta \leqslant 165$); f_a^S: alkylated aromatic C ($139 \leqslant \delta \leqslant 152$); f_a^B: aromatic bridgehead C ($129 \leqslant \delta \leqslant 139$); f_{al}*: CH_3 or quaternary C ($\delta = 16$); f_{al}^H: CH or CH_2 ($\delta = 30$); f_{al}^O: aliphatic C bonded to oxygen ($75 \leqslant \delta \leqslant 90$).

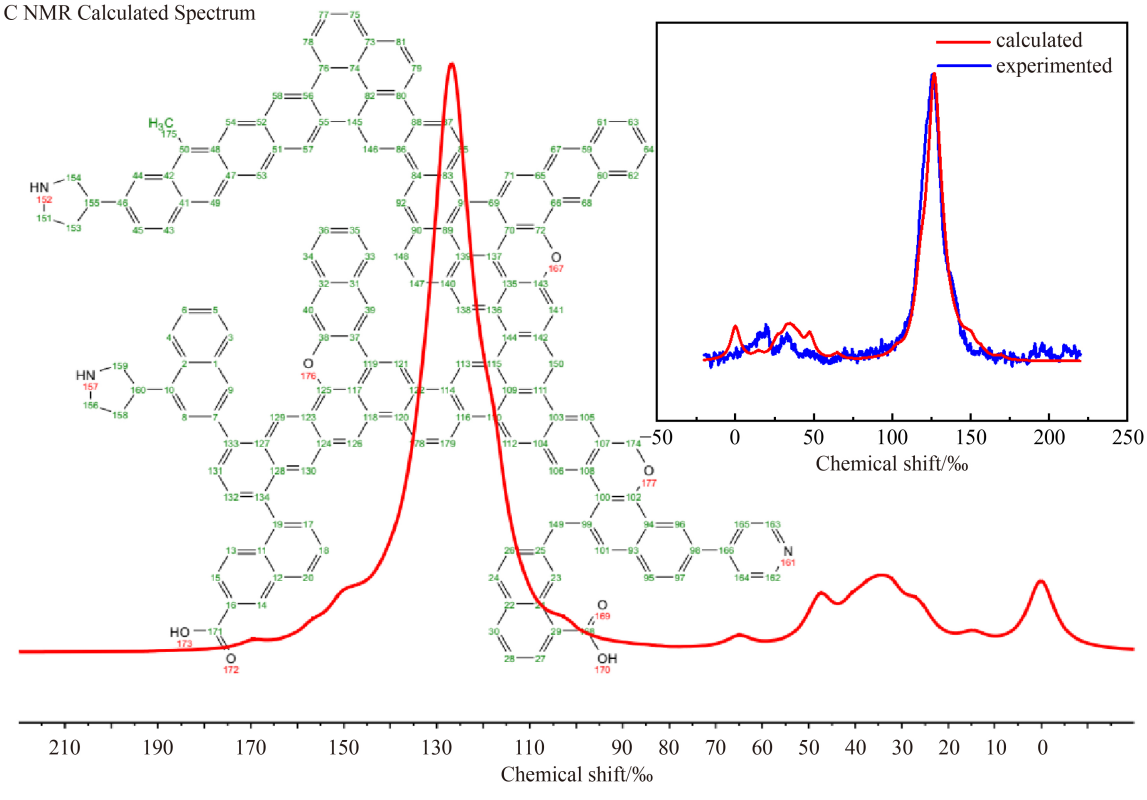

Fig. 2 Macromolecular structure and NMR spectrum of CP coal.

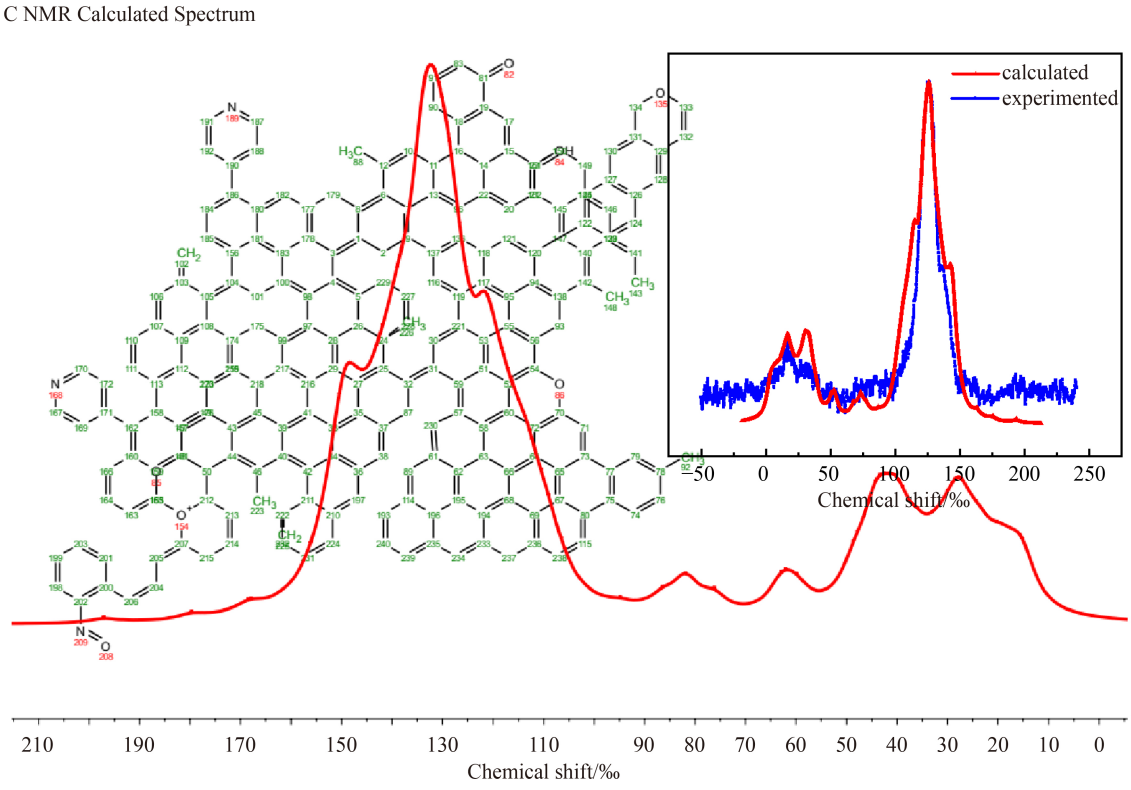

Fig. 3 Macromolecular structure and NMR spectrum of SH coal.

Table 3 Planar macromolecular structure model parameters

Coal sample number	Element content	Molecular formula	Molecular mass
CP	C (88.65%) H (4.62%) N (1.84%) O (4.89%)	$C_{169}H_{105}N_3O_7$	2289
SH	C (90.35%) H (4.62%) N (1.37%) O (3.66%)	$C_{230}H_{140}N_3O_7$	3057

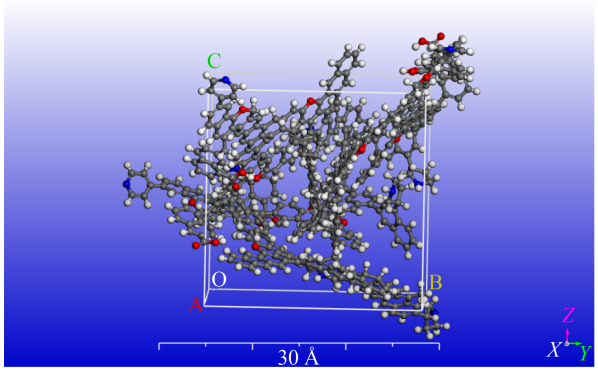

Fig. 4 Molecular structure model of CP coal after optimization.

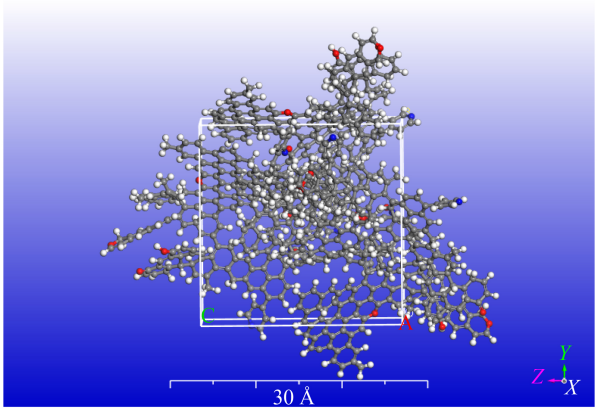

Fig. 5 Optimized molecular structure model of SH coal.

3.3 Microscopic mechanism of methane adsorption by coal structure

3.3.1 The action mechanism of molecular structure on methane

1) Effect of pore structure on methane adsorption

The adsorption conformation of CP molecular structure is shown in Fig. 7.

As shown in Fig. 7, CH_4 is mainly adsorbed in CI to CV-type pores in CP coal. The CI pore is U-shaped and adsorbs nine CH_4 molecules. The pore includes the pyrrole nitrogen CI_1, pyrrole nitrogen CI_2, and aromatic-ring structure + oxygen-containing functional group CI_3, with values of $E_{CH_4\text{-coal}}$ of −0.65, −1.33, and −1.71 kcal/mol, respectively.

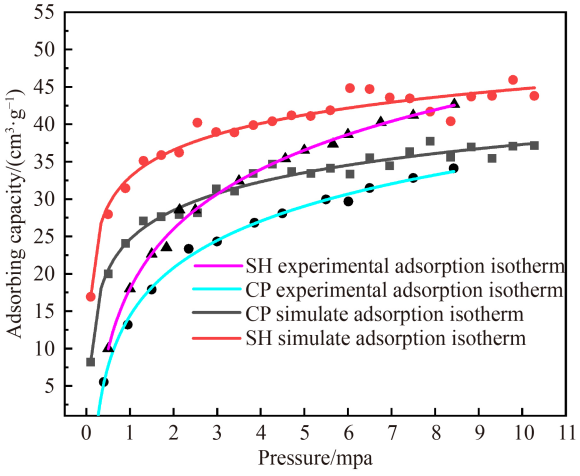

Fig. 6 Comparison of simulated and experimental isothermal adsorption curves

The CII pore, a L-shaped narrow pore, adsorbs four CH_4 molecules and comprises pyrrole nitrogen CII_1 and aromatic-ring structure CII_2. E_{CH_4-coal} values are (separately) −0.90 and −1.29 kcal/mol.

The CIII pore is classified as a K-type narrow pore that adsorbs eight CH_4 molecules and it consists of the aromatic-ring structure + oxygen-containing functional group $CIII_1$, aromatic-ring structure $CIII_2$, and pyrrole nitrogen $CIII_3$. Their E_{CH_4-coal} values are −0.66, −3.81, and −1.41 kcal/mol, respectively.

CIV denotes a connected pore of irregular shape that adsorbs six CH_4 molecules and consists of the aromatic-ring structure CIV_1, aromatic-ring structure + oxygen-containing functional group + aliphatic structure CIV_2, and aromatic-ring structure CIV_3, with E_{CH_4-coal} values of −0.99, −3.16, and −1.28 kcal/mol, respectively.

CV is a vase-shaped connected pore with a quadrilateral mouth; it adsorbs eight CH_4 molecules. The pore includes the aromatic-ring structure CV_1, aromatic-ring structure + pyrrole nitrogen CV_2 and aromatic-ring structure + aliphatic structure + pyrrole nitrogen CV_3, with values of E_{CH_4-coal} of −2.42, −4.53, and −3.25 kcal/mol, respectively.

The adsorption conformation of SH molecular structure is shown in Fig. 8.

Figure 8 reveals that CH_4 is mainly adsorbed in SI to SIII pores in SH coal. The SI connected pore adsorbs 18 CH_4 molecules in total and it comprises an aromatic-ring structure + oxygen-containing functional group + aliphatic structure SI_1, aromatic-ring structure + pyridine nitrogen SI_2, and aromatic-ring structure + oxygen-containing functional group SI_3. The values of E_{CH_4-coal} thereof are −3.45, −3.60, and −3.43 kcal/mol, respectively.

SII is an L-shaped pore that is narrow in the vertical direction and wide at the bottom, in which seven CH_4 molecules are adsorbed. The pore includes an aromatic-ring structure + aliphatic structure SII_1, aromatic-ring structure + oxygen-containing functional group SII_2, and aromatic-ring structure + pyridine nitrogen SII_3. The E_{CH_4-coal} values thereof are −1.61, −2.85, and −3.13 kcal/mol, respectively.

SIII is a lenticular pore and adsorbs one CH_4 molecule, including the aromatic-ring structure + aliphatic structure $SIII_1$, and $SIII_2$. The E_{CH_4-coal} values are (separately) −1.25 and −0.04 kcal/mol.

2) Interaction energy between molecular structures of coal and CH_4

E_{CH_4-coal} data in Tables 4 and 5 were analyzed by using the following methods of calculation.

① By calculating the average interaction energy of CII_2, $CIII_2$, CIV_1, CIV_3, and CV_1 structures, the average interaction energy of the aromatic-ring structure is −1.96 kcal/mol.

② By averaging Interaction energy of CI_1, CI_2, CII_1, and $CIII_3$ structures, the average interaction energy of the pyrrole nitrogen is −1.05 kcal/mol.

③ According to SI_2 and SII_3 structures, the average interaction energy of the aromatic-ring structure + pyridine nitrogen is −3.37 kcal/mol. Then, after subtracting the average interaction energy of aromatic-ring structures, the

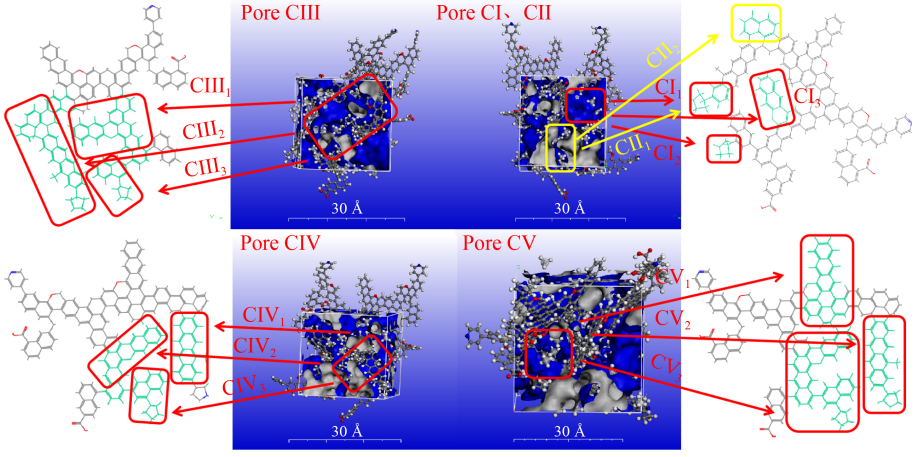

Fig. 7 Adsorption conformation of methane by molecular structure of CP coal.

Table 4 CP methane saturated adsorption pore structure parameters table

Serial number		Pore pattern	Pore structure	r(Å)	Methane adsorption number	$E_{CH_4\text{-coal}}$ /(kcal·mol^{-1})
CI	CI1	U-shaped pore	pyrrole nitrogen	3.83	2	−0.56
	CI2		pyrrole nitrogen	3.99	3	−1.33
	CI3		aromatic-ring structure + oxygen-containing functional group	5.56	4	−1.71
CII	CII1	L-shaped narrow pore	pyrrole nitrogen	5.57	2	−0.90
	CII2		aromatic-ring structure	4.31	2	−1.29
CIII	CIII1	K-type narrow pore	aromatic-ring structure + oxygen-containing functional group	7.32	2	−0.66
	CIII2		aromatic-ring structure	4.47	4	−3.81
	CIII3		pyrrole nitrogen	4.28	2	−1.41
CIV	CIV1	connected pore of irregular shape	aromatic-ring structure	6.13	1	−0.99
	CIV2		aromatic-ring structure + oxygen-containing functional group + aliphatic structure	3.80	4	−3.16
	CIV3		aromatic-ring structure	4.49	1	−1.28
CV	CV1	vase-shaped connected pore	aromatic-ring structure	4.89	2	−2.42
	CV2		aromatic-ring structure + pyrrole nitrogen	4.60	3	−4.53
	CV3		aromatic-ring structure + aliphatic structure + pyrrole nitrogen	4.67	3	−3.25

Note: Interaction energy is negative to indicate the adsorption force between the structure and methane.

Table 5 Pore structure parameters of SH methane saturation adsorption

Serial number		Pore pattern	Pore structure	r(Å)	Methane adsorption number	$E_{CH_4\text{-coal}}$ /(kcal·mol^{-1})
SI	SI_1	connected pore of U-shaped pore	aromatic-ring structure + oxygen-containing functional group + aliphatic structure	4.57	6	−3.45
	SI_2		aromatic-ring structure + pyridine nitrogen	4.51	6	−3.60
	SI_3		aromatic-ring structure + oxygen-containing functional group	4.95	6	−3.43
SII	SII_1	L-shaped pore	aromatic-ring structure + aliphatic structure	3.86	1	−1.61
	SII_2		aromatic-ring structure + oxygen-containing functional group	4.95	3	−2.85
	SII_3		aromatic-ring structure + pyridine nitrogen	4.78	3	−3.13
SIII	$SIII_1$	lenticular pore	aromatic-ring structure + aliphatic structure	4.75	1	−1.25
	$SIII_2$		aromatic-ring structure + aliphatic structure	9.17	1	−0.04

Note: Interaction energy is negative to indicate the adsorption force between the structure and methane.

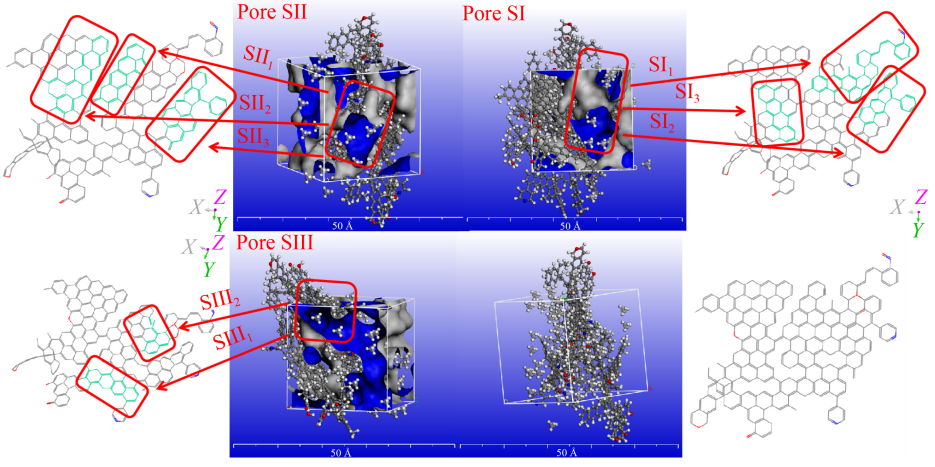

Fig. 8 Conformation of methane adsorption by SH coal molecular structure.

average interaction energy of the pyridine nitrogen is −1.41 kcal/mol.

④ Based on the average interaction energy of CI_3, $CIII_1$, SI_3, and SII_2 structures, the average interaction energy of the aromatic-ring structure + oxygen-containing functional group is −2.16 kcal/mol. The average interaction energy of oxygen-containing functional groups is −0.20 kcal/mol (after subtracting that of the aromatic-ring structure).

⑤ By subtracting the average interaction energy of pyridine nitrogen CV_3, the average interaction energy of the aromatic-ring structure + aliphatic structure is −2.20 kcal/mol. After removing the oxygen-containing functional group, the average interaction energies of aromatic-ring structures + aliphatic structures CIV_2 and SI_1 are −2.96 and −3.25 kcal/mol, respectively. Finally, by averaging with the interaction energies of SII_1 and $SIII_1$, the aromatic-ring structure + aliphatic structure is found to have a mean average interaction energy of −2.25 kcal/mol. After removing the aromatic-ring structure, the average interaction energy of the aliphatic structure is −0.29 kcal/mol.

The interaction energy between coal molecular structure and methane is shown in Fig. 9.

Figure 9 illustrates that the aromatic-ring structure, pyridine nitrogen, pyrrole nitrogen, aliphatic structure, and oxygen-containing functional group are ranked (in descending order) according to interaction energy.

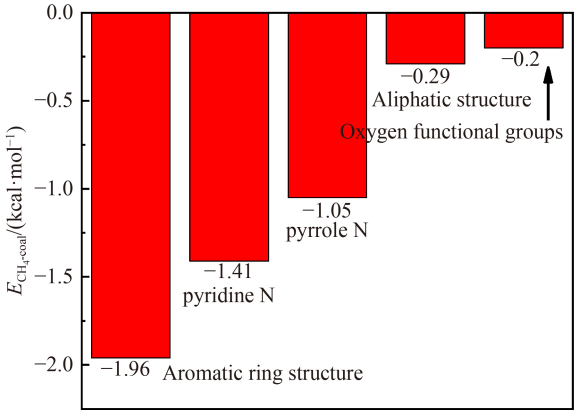

Fig. 9 Comparison diagram of interaction energy.

3.3.2 The mechanism of the effect of pore morphology on methane

1) Distribution state of methane molecules in CP coal

The distribution of methane molecules in pores CI to CV of CP coal is shown in Fig. 10.

Figure 10 indicates that CH_4 molecules adsorbed in the CI pore are mainly distributed around the turning part of the U-shaped pore and the lower part of the turning comprises pyrrole nitrogen CI_1 and CI_2, while the upper part consists of the aromatic-ring structure + oxygen-containing functional group CI_3.

CH_4 molecules adsorbed in the CII pore are mainly distributed around the turning end of the L-shaped pores, where the aromatic-ring structure CII_2 and pyrrole nitrogen CII_1 are shown.

CH_4 molecules adsorbed in the CIII pore are mainly found at the K-shaped turning part, where it is composed of the aromatic-ring structure + oxygen-containing functional group $CIII_1$ and pyrrole nitrogen $CIII_3$. The aromatic-ring structure $CIII_2$ is mainly found in a straight section of the CIII pore.

In the CIV pore, CH_4 molecules are mainly distributed around the center surrounded by three structures, i.e., CIV_1, aromatic-ring structure in CIV_2, and CIV_3.

In the CV pore, CH_4 molecules are uniformly arranged within the irregular pore and are surrounded by CV_1, by pyrrole nitrogen in CV_2, and the aliphatic structure in CV_3.

2) Distribution of CH_4 molecules in SH coal

The distribution of CH_4 molecules in SI to SIII pores in SH coal is displayed in Fig. 11.

Figure 11 shows that more CH_4 molecules are adsorbed

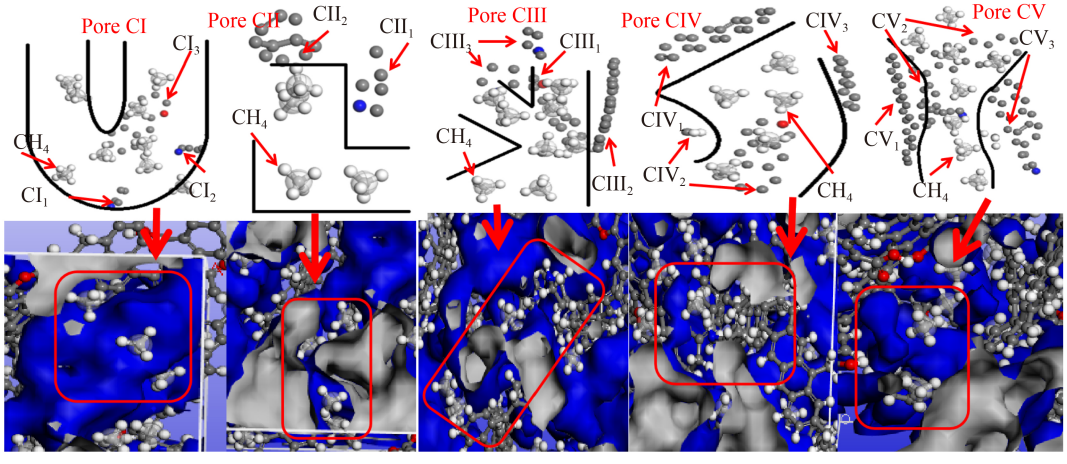

Fig. 10 Methane distribution in CP coal.

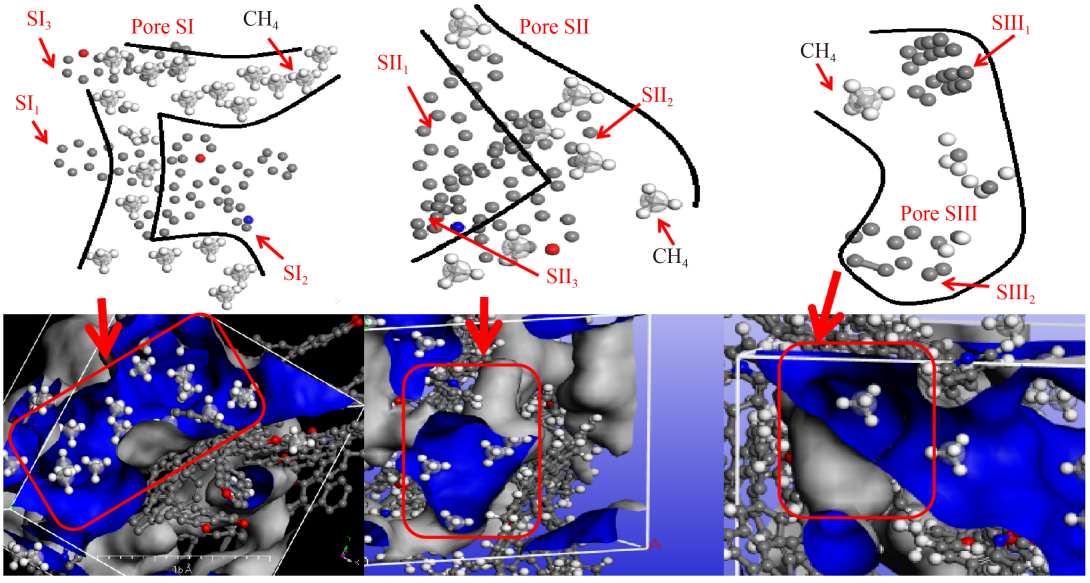

Fig. 11 Methane distribution in SH coal.

in the SI pore and they are mainly concentrated near the aromatic-ring structures in SI_1, SI_2, and SI_3.

Only a few CH_4 molecules are adsorbed in the SII pore; these are mainly concentrated near the aromatic-ring structures in SII_1, SII_2, and SII_3.

In the SIII pore, few CH_4 molecules are adsorbed; these are mainly concentrated near the aromatic-ring structure in $SIII_1$.

3.4 Uncertainty analysis

1) This paper only studies the medium and high rank coals of Changping coal and Sihe coal, but not discuss the low rank coals. There are considerable differences in the characteristics of coal pore fissure of different rank coals, so the pore characteristics of low rank coals cannot be characterized.

2) Due to the strong heterogeneity of coal samples and the limitation of computer memory, the grand canonical Monte Carlo simulation used in this paper has a certain randomness, resulting in a certain difference between the simulated calculation results and the measured results.

3) Coal matrix is composed of thousands of coal molecules. In this paper, the macromolecular structure model of coal was constructed based on the test samples, and the adsorption mechanism of methane was studied. The diversity of pore types leads to differences in coal molecular structure and morphology, which needs further research in the future.

4 Conclusions

1) Based on elements, FTIR, XPS, and ^{13}C NMR, the macromolecular structure models of CP semi-anthracite and SH anthracite were optimized and established. Isothermal adsorption experiments and GCMC simulation methods were used to obtain the adsorption curves in accordance with the Langmuir model. The V_L of CP and SH coal experiments is 34 cm^3/g and 42 cm^3/g, and the simulated values of V_L are 37 cm^3/g and 43 cm^3/g.

2) The molecular structure composition of CP and SH coals and the strength of adsorption interaction between methane and coal structure were evaluated. The aromatic-ring structure (1.96 kcal/mol), pyridine nitrogen (1.41 kcal/mol), pyrrole nitrogen (1.05 kcal/mol), aliphatic structure (0.29 kcal/mol), and oxygen-containing functional group (0.20 kcal/mol) were ranked (in descending order) according to the adsorption force between these molecular structures in coal and CH_4.

3) The position at which CH_4 is adsorbed in semi-anthracite and anthracite mainly depends on the positions of aromatic-ring structures, pyrrole nitrogen, and pyridine nitrogen. Its degree of aggregation is commonly affected by interaction energy and pore morphology. CH_4 is mainly accumulated at positions where the pore morphonology changes (such as at the turning parts and turning points of a pore).

Acknowledgement This study was supported by the National Natural Science Foundation of China (Grant Nos. 41872174 and 42072189) and the Program for Innovative Research Team (in Science and Technology) in Universities of Henan Province, China (No. 21IRTSTHN007) and the Program for Innovative Research Team (in Science and Technology) of Henan Polytechnic University (No.T2020-4).

References

Bin Z, Zeng F G, Wang D Z, Kang G X, Zhang X Y, Kang T H (2021). Macromolecular structure model of anthracite in southern Qinshui

Basin andits methane bearing mechanical properties. J China Coal Soc, 46(02): 534–543

Brochard L, Vandamme M, Pellenq R J M, Fen-Chong T (2012). Adsorption-induced deformation of microporous materials: coal swelling induced by CO_2-CH_4 competitive adsorption. Langmuir, 28(5): 2659–2670

Dong Y, Ju B, Zhang S, Tian Y, Ma S, Liu N, Lu G (2020). Microscopic mechanism of methane adsorption in shale: experimental data analysis and interaction potential simulation. J Petrol Sci Eng, 184: 106544

Du X, Cheng Y, Liu Z, Yin H, Wu T, Huo L, Shu C (2021). CO_2 and CH_4 adsorption on different rank coals: a thermodynamics study of surface potential, Gibbs free energy change and entropy loss. Fuel, 283: 118886

Jiang J Y, Yang W H, Cheng Y P, Liu Z D, Zhang Q, Zhao K. (2019). Molecular structure characterization of middle-high rank coal via XRD, Raman and FTIR spectroscopy: implications for coalification. Fuel, 239: 559–572

Kazemi M, Takbiri-Borujeni A (2017). Modeling and simulation of gas transport in carbon-based organic nano-capillaries. Fuel, 206: 724–737

Kurniawan Y, Bhatia S K, Rudolph V (2006). Simulation of binary mixture adsorption of methane and CO_2 at supercritical conditions in carbons. AIChE J, 52(3): 957–967

Li Y X, Hu Z M, Liu X G, Gao S, Duan X, Chang J, Wu J (2018). Insights into interactions and microscopic behavior of shale gas in organic−rich nano−slits by molecular simulation. J Nat Gas Sci Eng, 59: 309–325

Liu X, Song D, He X, Nie B, Wang Q, Sun R, Sun D (2018). Coal macromolecular structural characteristic and its influence on coalbed methane adsorption. Fuel, 222: 687–694

Men X Y, Tao S, Liu Z X, Tian W G, Chen S (2021). Experimental study on gas mass transfer process in a heterogeneous coal reservoir. Fuel Process Technol, 216: 106779

Meng Z, Liu S, Li G (2016). Adsorption capacity, adsorption potential and surface free energy of different structure high rank coals. J Petrol Sci Eng, 146: 856–865

Mosher K, He J, Liu Y, Rupp E, Wilcox J (2013). Molecular simulation of methane adsorption in micro- and mesoporous carbons with applications to coal and gas shale systems. Int J Coal Geol, 109-110: 36−44

Shang Z, Dong L, Niu L, Shi H (2019). Adsorption of methane, nitrogen, and carbon dioxide in atomic-scale fractal nanopores by Monte Carlo simulation I: single-component adsorption. Energy Fuels, 33(11): 10457–10475

Song W, Yao J, Ma J, Li A, Li Y, Sun H, Zhang L (2018). Grand canonical Monte Carlo simulations of pore structure influence on methane adsorption in micro-porous carbons with applications to coal and shale systems. Fuel, 215: 196–203

Sposito G, Park S H, Sutton R (2000). Monte Carlo simulation of the total radial distribution function for interlayer water in sodium and potassium montmorillonites. Clays Clay Miner, 47(2): 192–200

Tao G, Yang L, Meng W, Fen L, Zhang M (2020). Structural characterization and molecular model construction of gas-fat coal with high sulfur in Shanxi. Spectrosc Spectral Analysis, 40(11): 3373–3378

Tao S, Zhao X, Tang D Z, Deng C M, Meng Q, Cui Y (2018). A model for characterizing the continuous distribution of gas storing space in low-rank coals. Fuel, 233: 552–557

Tao S, Pan Z J, Chen S D, Tang S L (2019). Coal seam porosity and fracture heterogeneity of marcolithotypes in the Fanzhuang Block, southern Qinshui Basin, China. J Nat Gas Sci Eng, 66: 148–158

Wang K, Zhang B, Kang T (2020). Effect of geological depths on CH4adsorption,diffusion, and swelling in kaolinite by molecular simulations. Energy Fuels, 34(2): 1620–1626

Yan J, Lei Z, Li Z, Wang Z, Ren S, Kang S, Wang X, Shui H (2020). Molecular structure characterization of low-medium rank coals via XRD, solid state 13C NMR and FTIR spectroscopy. Fuel, 268: 117038

Yeganegi S, Gholampour F (2016). Simulation of methane adsorption and diffusion in a carbon nanotube channel. Chem Eng Sci, 140: 62–70

Zhao Y, Mei-fen L I, Zeng F (2018). FTIR study of structural characteristics of different chemical components from Yimin Lignite. J China Coal Soc, 43(02): 546–554